Second Virial Coefficient for Pure HFC Refrigerants and their Mixtures+R744 - Theoretical Calculations in Comparison with Experimental Data[1]

Jurij Avsec[2,4], Giovanni Di Nicola[3], Milan Marcic[2], Fabio Polonara[3]

[1]Paper presented at the Fifteenth Symposium on Thermophysical Properties, June 22-27, 2003, Boulder, Colorado U.S.A.

[2]University of Maribor, Faculty of Mechanical Engineering, Smetanova 17, 2000 Maribor, P.O. BOX 224, SLOVENIA; Email: jurij.avsec@uni-mb.si

[3]Dipartimento di Energetica, Università di Ancona, Via Brecce Bianche, 60100 Ancona, Italy

[4]To whom corresspondence should be addresseed. Email: jurij.avsec@uni-mb.si

ABSTRACT

The paper features the mathematical model of computing the second virial coefficient for HFC refrigerants+R744 on the basis of statistical thermodynamics. In the present paper we have developed the new model for calculation of second virial coefficient which yields favorable results in practical computations for a large number of components and within a relatively wide range of densities and temperatures. We consider rigid nonlinear molecules with the reference Lennard-Jones interaction potential and dipole and quadrupole moment. The constants necessary for the computation like the characteristic temperatures of rotation, electronic state etc. and the inertia moments are obtained analytically applying the knowledge of the atomic structure of the molecule.

The second virial coefficients for mixtures are obtained using the one-fluid theory. For the mixtures we have developed the original mixing rules. We have developed also new mixing rules for dipole and quadrupole moments.

In this work, the virial coefficients for the pure refrigerants R125, R32, R744 and mixtures R125+CO_2, R32+CO_2, measured by means of Burnett apparatus were analyzed. The experimental uncertainty in second virial coefficient was estimated to be ± 2 cm^3/mol by average. The analytical results are compared with the experimental data obtained by Burnett apparatus and they show a very good agreement.

Keywords: Second virial coefficient, statistical thermodynamics, refrigerants

1. INTRODUCTION

In engineering practice in most cases the thermodynamic tables or diagrams or different empirical functions obtained from measurement are used (classical thermodynamics). Today, there are numerous equations of state (EOS) reported in the literature for describing the behaviour of fluids: Van der Waals EOS (VDW), Peng-Robinson (PR), Redlich-Kwong EOS (RK), Soave EOS … [1]. However, these equations have exhibited some noticeable defects, such as poor agreement with experimental data at moderate densities. On the other side, we can use the complex equations of state with many constants (Benedict-Webb-Rubin [1] (BWR) EOS, Lee-Kessler [1] EOS, Benedict-Webb-Rubin-Starling-Nishiumi [1] EOS (BWRSN), Jacobsen-Stewart [2] EOS (JS), Tillner-Roth-Watanabe-Wagner [3] EOS (TRWW), Jacobsen-Lemmon [4] EOS (JL)…). These equations are more complicated. They have no insight into the microstructure of matter and poor agreement with experimental data outside the interpolation limits.

2. COMPUTATION OF THERMODYNAMIC PROPERTIES OF THE STATE

To calculate thermodynamic functions of state we applied the canonical partition function [5]. Utilising the semi-classical formulation for the purpose of the canonical ensemble for the N indistinguishable molecules the partition function Z can be expressed as follows:

$$Z = \frac{1}{N!\,h^{Nf}} \int ..\int \exp\left(-\frac{H}{kT}\right) \cdot d\vec{r}_1 d\vec{r}_2 ..d\vec{r}_N d\vec{p}_1 d\vec{p}_2 ..d\vec{p}_N \qquad (1)$$

where f stands for the number of degrees of freedom of an individual molecule, H designates the Hamiltonian molecule system, vectors $\vec{r}_1, \vec{r}_2 .. \vec{r}_N$ describe the positions of N molecules and $\vec{p}_1, \vec{p}_2 ... \vec{p}_N$ momenta, k is the Boltzmann`s constant and h is the Planck`s

constant. The canonical ensemble of partition function for the system of N molecules can be expressed by:

$$Z = Z_0 Z_{trans} Z_{vib} Z_{rot} Z_{ir} Z_{el} Z_{nuc} Z_{conf} \quad (2)$$

Thus the partition function Z is a product of terms of the ground state (0), the translation (trans), the vibration (vib), the rotation (rot), the internal rotation (ir),the influence of electrons excitation (el), the influence of nuclei excitation (nuc) and the influence of the intermolecular potential energy (conf).

3. INFLUENCE OF LENNARD-JONES INTERMOLECULAR POTENTIAL

3.1. Johnson-Zollweg-Gubbins (JZG) model [6].

For a real fluid the Johnson-Zollweg-Gubbins (1993) model based on molecular dynamic and Monte Carlo simulations with the Lennard-Jones intermolecular potential is possible to use. The MBWR EOS contains 32 linear parameters (x_i) and one non-linear parameter (γ).

On this basis we can express configurational free energy A_{conf}:

$$A_{conf}^{*} = \sum_{i=1}^{8} \frac{a_i \rho^{*i}}{i} + \sum_{i=1}^{6} b_i G_i \,, \quad (3)$$

where the coefficients a_i, b_i and G_i are presented in the literature [6]. The coefficients a_i and b_i are solely functions of the reduced temperature T^*, the coefficients G_i are functions of the reduced density ρ^* and of the nonlinear adjustable parameter γ.

$$\rho^{*} = \frac{N\sigma^3}{V}, \qquad T^{*} = \frac{kT}{\varepsilon}, \qquad A_{conf}^{*} = \frac{A_{conf}}{N\varepsilon} \quad (4)$$

$$F = \exp\left(-\gamma \rho^{*2}\right) \qquad , \ \gamma=3 \quad (5)$$

where A_{conf} is reduced configurational free energy, σ and ε are Lennard-Jones parameters.

4. IMPACT OF ANISOTROPIC POTENTIALS ON THERMODYNAMIC FUNCTIONS OF STATE

There are several methods to compute the influence of anisotropic potentials [5-12]. In the present paper those models were used which yielded favorable results in practical computations for a large number of components and within a relatively wide range of densities and temperatures.

4.1 Lucas-Gubbins's model (LG) [5,8].

The Lucas-Gubbins's model deals with the perturbation expansion around the Lennard-Jones's intermolecular potential. The total intermolecular potential can be written as a sum of the Lennard-Jones's intermolecular potential (LJ) and the potential, which takes into account also the orientation of a molecule in space (p):

$$u_{12}(r_{12},\omega_1,\omega_2) = u_{12}^{LJ}(r_{12}) + u_{12}^{p}(r_{12},\omega_1,\omega_2) \tag{6}$$

In Eq. (6), r_{12} is the distance of centers of gravity between the molecules 1 and 2, ω_1 and ω_2 are orientations of both molecules in space, which may be expressed with Euler's angles (ϕ,ϑ,χ). The reference part u^{LJ} can be written also as a certain mean intermolecular energy at the distance r_{12}:

$$u_{12}^{LJ}(r_{12}) = \langle u_{12}(r_{12},\omega_1,\omega_2)\rangle_{\omega_1\omega_2} = \frac{\int u_{12}(r_{12},\omega_1,\omega_2)d\omega_1 d\omega_2}{\int d\omega_1 d\omega_2} \tag{7}$$

Now suppose that the sum of intermolecular potential energy is:

$$U_{conf} = \sum_{i<j} u_{ij} = \sum_{i<j} u_{ij}^{LJ}(r_{12}) + \sum_{i<j} u_{ij}^{p}(r_{12},\omega_1,\omega_2) \tag{8}$$

Using the perturbation expansion around the reference potential one can then write the configuration effect to the free energy as:

$$\frac{A_{conf}}{Nk_BT} = \frac{A^{LJ}}{Nk_BT} + \frac{A^{\lambda}}{Nk_BT} + \frac{A^{\lambda\lambda}}{Nk_BT} + \frac{A^{\lambda\lambda\lambda}}{Nk_BT} \quad (9)$$

The free energy of Lennard-Jones's fluid A^{LJ} was calculated using the Johnson-Zolweg-Gubbins's (JZG) model [6].

We consider rigid nonlinear molecules [6] with the assumption that all anisotropic interactions are scalars. The multipole expansion is terminated at the octopole term. Intermolecular repulsion interaction is modelled by the Lennard-Jones r^{-12} law. The induction interaction are formulated in the isotropic polarizibility approximation. Intermolecular interactions are limited to the second-order term, cross terms between intemolecular interactions are not considered. The configurational free energy is then given by:

First order terms:

Inductive forces:

$$\left(A^{\lambda}\right)^{ind} = -4\pi N\rho\alpha\left(\mu^2\right)\frac{J(6)}{\sigma^3} - 6\pi N\rho\alpha\left(\theta^2\right)\frac{J(8)}{\sigma^5} \quad (10)$$

Second order terms:

Multipole forces:

$$\left(A^{\lambda\lambda}\right)^{mult-mult} = \left(A(112)^{\lambda\lambda}\right)^{mult-mult} + 2\left(A(123)^{\lambda\lambda}\right)^{mult-mult} + \left(A(224)^{\lambda\lambda}\right)^{mult-mult} \quad (11)$$

$$\left(A(112)^{\lambda\lambda}\right)^{mult-mult} = -\frac{2}{3}\frac{\pi N\rho}{k_BT}\frac{\mu^4}{\sigma^3}J(6) \quad (12)$$

$$\left(A(123)^{\lambda\lambda}\right)^{mult-mult} = -\frac{\pi N\rho}{k_BT}\frac{\mu^2\theta^2}{\sigma^5}J(8) \quad (13)$$

$$\left(A(224)^{\lambda\lambda}\right)^{mult-mult} = -\frac{14}{5}\frac{\pi N\rho}{k_BT}\frac{\theta^4}{\sigma^7}J(10) \quad (14)$$

If the intermolecular potential is restricted to the dipole-dipole term, Eq. (12) is the only contribution, while for quadrupolar (CO_2, C_2H_6, etc.) molecules Eq. (14) is the only non vanishing term. For tetrahedral molecules (CH_4, CCl_4, CF_4, etc.) the leading multipole term is the octopole-octopole and the corresponding contribution to free energy is:

$$\left(A(336)^{\lambda\lambda}\right)^{\text{mult-mult}} = -\frac{19008}{875}\frac{\pi N\rho}{k_B T}\frac{\Omega^4}{\sigma^{11}}J(14) \tag{15}$$

Dispersion forces

$$\left(A(202+022)^{\lambda\lambda}\right)^{\text{disp-disp}} = -\frac{32\pi N\rho}{5k_B T}\sigma^3\varepsilon^2\kappa^2 J(12) - \frac{16\pi^2 N\rho^2}{5k_B T}\varepsilon^2\sigma^6\kappa^2 L(662) \tag{16}$$

$$\left(A(224)^{\lambda\lambda}\right)^{\text{disp-disp}} = -\frac{10368\pi N\rho}{875k_B T}\sigma^3\varepsilon^2\kappa^4 J(12) \tag{17}$$

Third order terms:

$$\begin{aligned}\left(A_A{}^{\lambda\lambda}\right)^{\text{mult-mult-mult}} &= 3\left(A_A(112;112,224)^{\lambda\lambda\lambda}\right) + 6\left(A_A(112;123;213)^{\lambda\lambda\lambda}\right) + \\ &6\left(A_A(123;123;224)^{\lambda\lambda\lambda}\right) + \left(A_A(224;224;224)^{\lambda\lambda\lambda}\right)\end{aligned} \tag{18}$$

$$\left(A_A(112;123;213)^{\lambda\lambda\lambda}\right) = \frac{8\pi N\rho}{25(k_B T)^2}\frac{\mu^4\theta^2}{\sigma^8}J(11) \tag{19}$$

$$\left(A_A(112;123;213)^{\lambda\lambda\lambda}\right) = \frac{8\pi N\rho}{75(k_B T)^2}\frac{\mu^4\theta^2}{\sigma^8}J(11) \tag{20}$$

$$\left(A_A(123;123;224)^{\lambda\lambda\lambda}\right) = \frac{8\pi N\rho}{35(k_B T)^2}\frac{\mu^2\theta^4}{\sigma^{10}}J(13) \tag{21}$$

$$\left(A_A(224;224;224)^{\lambda\lambda\lambda}\right) = \frac{144\pi N\rho}{245(k_B T)^2}\frac{\theta^6}{\sigma^{12}}J(15) \tag{22}$$

$$\begin{aligned}\left(A_B{}^{\lambda\lambda}\right)^{\text{mult-mult-mult}} &= \left(A_B(112;112,112)^{\lambda\lambda\lambda}\right) + 3\left(A_B(123;123;224)^{\lambda\lambda\lambda}\right) + \\ &3\left(A_B(123;123;224)^{\lambda\lambda\lambda}\right) + \left(A_B(224;224;224)^{\lambda\lambda\lambda}\right)\end{aligned} \tag{23}$$

$$\left(A_B(112;112;112)^{\lambda\lambda\lambda}\right)=\frac{32\pi^3}{135}\left(\frac{14\pi}{5}\right)^{1/2}\frac{N\rho^2}{(k_BT)^2}\frac{\mu^6}{\sigma^3}K(222;333) \quad (24)$$

$$\left(A_B(112;123;123)^{\lambda\lambda\lambda}\right)=\frac{64\pi^3}{315}(3\pi)^{1/2}\frac{N\rho^2}{(k_BT)^2}\frac{\mu^4\theta^2}{\sigma^5}K(233;344) \quad (25)$$

$$\left(A_B(123;123;224)^{\lambda\lambda\lambda}\right)=-\frac{32\pi^3}{45}\left(\frac{22\pi}{63}\right)^{1/2}\frac{N\rho^2}{(k_BT)^2}\frac{\mu^2\theta^4}{\sigma^7}K(334;445) \quad (26)$$

$$\left(A_B(224;224;224)^{\lambda\lambda\lambda}\right)=\frac{32\pi^3}{2025}(2002\pi)^{1/2}\frac{N\rho^2}{(k_BT)^2}\frac{\mu^6}{\sigma^9}K(222;333) \quad (27)$$

When intermolecular potential is terminated at the dipole-dipole term the Eq. (24) is the only contributing term. Similarly, for quadrupolar fluids Eq. (27) is the only nonvanishing term. For tetrahedral molecules where the octopol-octopole potential is the lowest multipole term, the ($A_A^{\lambda\lambda\lambda}$) is zero and we can express contribution to free energy:

$$\left(A_B{}^{\lambda\lambda\lambda}\right)=\left(A_B(336;336;336)^{\lambda\lambda\lambda}\right)-\frac{221184\pi^3}{11375}\left(\frac{3533\pi}{737}\right)^{1/2}\frac{N\rho^2}{(k_BT)^2}\frac{\Omega^6}{\sigma^{15}}K(666,777) \quad (28)$$

The structural properties of the Lennard-Jones potential are introduced via J, L integrals [5]. The J, K and L integrals are calculated by numerical integration over tabulated pair correlation functions. We calculated the J, K and L integrals with help of simple interpolation equations:

Nicolas-Gubbins-Street-Tildesley (LG): interpolation limit: $0\le\frac{N\sigma^3}{V}\le 1.2,\ 0.5\le\frac{k_BT}{\varepsilon}\le 6$,

In thermodynamic perturbation theory from the properties of the real system we can obtain the Helmholtz free energy in powers of the perturbation potential (Eq. 9). When Eq. (9) is terminated at third-order term it is found that the results are good for moderate polar fluids but fail for strong dipoles (H_2O, NH_3…). Similar results have been found for quadrupole forces[27]. This is shown for a liquid state condition in Fig. Due to slow convergence of

Eq.(9) for strong multipole strengths the following simple Pade approximation for the free energy can be found in the literature[6,28]:

$$\frac{A_{conf}}{Nk_BT}=\frac{A^{LJ}}{Nk_BT}+\frac{A^{\lambda}}{Nk_BT}+\frac{A^{\lambda\lambda}}{Nk_BT}\left(1-\frac{A^{\lambda\lambda\lambda}}{A^{\lambda\lambda}}\right) \tag{29}$$

5. MIXING RULES

The thermodynamic properties of Lennard-Jones mixtures are obtained using the ome-fluid theory. The molecules interacting with Lennard-Jones potential have parameters σ and ε given by:

$$\sigma^3=\sum_{\alpha,\beta}\psi_\alpha\psi_\beta{\sigma_{\alpha\beta}}^3\ \varepsilon\sigma^3=\sum_{\alpha,\beta}\psi_\alpha\psi_\beta\varepsilon_{\alpha\beta}{\sigma_{\alpha\beta}}^3. \tag{30}$$

$$\sigma_{\alpha\beta}=\frac{\sigma_{\alpha\alpha}+\sigma_{\beta\beta}}{2},\varepsilon_{\alpha\beta}=\sqrt{\varepsilon_{\alpha\alpha}\varepsilon_{\beta\beta}}\ . \tag{31}$$

The dipole and quadrupole moments with the next are represented [13]:

$$\sigma^3\varepsilon^2\mu^4=\sum_{\alpha,\beta}\psi_\alpha\psi_\beta{\sigma_{\alpha\beta}}^3{\varepsilon_{\alpha\beta}}^2{\mu_\alpha}^2{\mu_\beta}^2 \tag{32}$$

$$\sigma^3\varepsilon^2\theta^4=\sum_{\alpha,\beta}\psi_\alpha\psi_\beta{\sigma_{\alpha\beta}}^3{\varepsilon_{\alpha\beta}}^2{\theta_\alpha}^2{\theta_\beta}^2 \tag{33}$$

The formulation of octopole moment is new and is formulated on analogy of dipole and quadrupole moments.

$$\sigma^3\varepsilon^2\Omega^4=\sum_{\alpha,\beta}\psi_\alpha\psi_\beta{\sigma_{\alpha\beta}}^3{\varepsilon_{\alpha\beta}}^2{\Omega_\alpha}^2{\Omega_\beta}^2 \tag{34}$$

6. SECOND VIRIAL COEFFICIENTS OF POLAR SUBSTANCES

Calculation of second virial coefficients for real substances is possible by the classical [16-35] and statistical thermodynamics [15-25]. Classical thermodynamics has no insight into

the microstructure of the substance. But it allows the calculation of thermodynamics function of state with asistance of measurement or empirical equations. Statistical thermodynamics, on the other hand, calculates the properties of state on the basis of molecular motions in a space, and on the basis of the intermolecular interactions.

The virial equation of state is the expansion of the compressibility factor Z_r along individual isotherms in terms of density around acoording to the next equation:

$$Z_r = \frac{pV}{NkT} = 1 + \frac{B}{V} + \frac{C}{V^2} ..... \tag{35}$$

where B and C are second and third virial coefficient and the are defined as:

$$B = \left(\frac{\partial Z_r}{\partial n} \right)_{n=0}, \; C = \frac{1}{2!} \left(\frac{\partial^2 Z_r}{\partial n^2} \right)_{n=0} ,..... \tag{36}$$

The are properties of gas at n=0 and the do not depend on density, but only on temperature and, in mixtures, on composition.

From the MBWR EOS for LJ potential we with help of Eq. (3) obtain the next expression:

$$B_{LJ} = N_A \sigma^3 \left(x_1 + x_2 T^{*-1/2} + x_3 T^{*-1} + x_4 T^{*-2} + x_5 T^{*-3} \right) \tag{37}$$

The B_{ex} is the contribution of multipole moments through Pade approximation equation. It is the complex function in strong dependence of temperature and mixture composition. The second virial coefficient is then expressed with the next equation:

$$B = B_{LJ+B_{ex}} \tag{38}$$

7. EXPERIMENTAL SETUP

7.1. Apparatus.

It consists of two pressure vessels, the measurement chamber, V_A, and the expansion chamber, V_B, with a volume of approximately (70 and 35) cm^3, respectively, and some auxiliary systems for filling and mixing the compounds in the Burnett vessels and for controlling and measuring the pressure and temperature. The four-valve arrangement enables the vessels V_A and V_B to be filled or emptied separately and, in addition to the expansion experiment, allows for the compounds in the Burnett vessels to be mixed using a magnetic recirculating pump. The measurement vessel is connected to a diaphragm-type differential pressure transducer (Ruska Model 2413), which is coupled to an electronic null indicator (Ruska Model 2416).

The pressure is regulated by a precision pressure controller (Ruska Model 3981), while a digital pressure indicator (Ruska Model 7000) is used to measure pressures. Nitrogen is used to balance the sample gas pressure, and the nitrogen circuit consists of a reservoir, expansion vessels and pressure regulating systems.

The vessels are immersed in a thermostatic bath filled with about 45 liters of an ethylene glycol and water mixture. The temperature of the bath is kept constant by means of a system with a PID device, piloted by a computer to which the temperature measurement system is also connected. The temperature control and acquisition system relies on two platinum resistance thermometers calibrated according to ITS 90 at the Istituto Metrologico G. Colonnetti (IMGC), of Turin. In particular, for temperature measurements, a Hart Scientific Pt 25 Ω resistance thermometer (mod. Hart 5680) is used, while for control purposes a Tersid Pt 100 Ω resistance thermometer is used. Both the thermometers are connected to a digital temperature indicator (Corradi, RP 7000).

8. RESULTS AND DISCUSSION

We have carried out the calculations for pure refrigerants R125, R32 and R744 and refrigerant mixtures R125-R744 and R32-R744. The comparison of our calculations on the basis of statistical thermodynamics (JZG-LG model) with experimental results (Exp) are presented in tables 1-5.

Tables 1, 2 and 4 feature the second virial coefficient for pure refrigerants R125, R32 and R744 as the function of relative deviation (RD) in the real gas region. The maximum relative deviation of the JZG-LG model from the TRWW model is less than 10% in comparison with experimental data.

Tables 3 and 5 show the RD of the second virial coefficient for mixtures R125-R744 and R32-R744 for the real gas region. The maximum RD from the experimental data is less than 11% in comparison with the calculated data.

CONCLUSION AND SUMMARY

The paper presents the mathematical model for computation of the second virial coefficient in the fluid region. For the real fluid, the Johnson-Zollweg-Gubbins model based on molecular dynamic and Lennard-Jones simulations and modified Benedict-Webb-Rubin equation of state (MBWR) was applied. In this paper are multipolar and induction interactions calculated with help of quantum mechanical calculation of the intermolecular energy function with help of Lucas-Gubbins perturbation theory. The multipole expansion is terminated at the octopole term. The analytical results are compared with the experimental data and they show a very good agreement.

REFERENCES

1. S.M. Walas, *Phase Equilibria in Chemical Engineering*, (Buttenworth Publishers, Boston, 1984)

2. R.T. Jacobsen, R.B. Stewart, M. Jahangiri, S.G. Penoncello, **31**:1161 (1986).

3. J. Li, R. Tillner-Roth, H. Sato, K. Watanabe, Fluid Phase Equilibria, **161**:225 (1999).

4. E.W. Lemmon, R.T. Jacobsen, International Journal of Thermophysics, **20**:825 (1999).

5. K. Lucas, *Applied Statistical Thermodynamics* (Springer-Verlag, New York, 1992).

6. L.K. Johnson, J.A. Zollweg, K.E. Gubbins, Molecular Physics, **78**:591 (1993).

7. Rigby, E.B. Smith, W.A. Wakeham, G.C. Maithland, *The Forces between Molecules*, (Clarendon Press, Oxford, 1986).

8. C.G. Gray, K.E. Gubbins*, Theory of Molecular Fluids* (Clarendon Press, Oxford, 1984).

9. C. Twu, K.E. Gubbins, Chemical Engineering Science, **33**:879 (1978).

10. C. Twu, K.E. Gubbins, Chemical Engineering Science, **33**:863 (1978).

12. B.J. Moser, *Die Theorie der Intermolekularen Wechseelwirkungen und Ihre Anwendung auf die Berechnung von Verdampfungsgleichgewichten binärer Systeme*", PhD Thsesis (Universität Duisburg, Germany, 1981).

13. J.L. Nicolas, K.E. Gubbins, W.B. Street, D.J. Tildesley, Molecular Physics **37**:1429 (1979).

14. U.Weingerl, M. Wedland, J. Fischer, A. Müller, A., J. Winkelman, AIChE Journal, **47**:705 (2002).

15. W.H. Keesom, *The Second Virial Coefficient for Rigid Spherical Molecules*, Communications from the Physical Laboratory, University of Leiden, Supplement No. 39[a], 1915, p.p. 1-16

16. J.S. Rowlinson, Trans. Faraday Soc.,**44**:120-127 (1951).

17. J.S. Rowlinson, Trans. Faraday Soc., **45**:974 (1949).

18. J.O. Hirschfelder, C.F. Curtiss, R.B. Bird,. *Molecular Theory of Gases and Liquids*, (John Willey & Sons, London, 1954)

19. J.O. Hirschfelder, F.T. McClure, I.F. Weeks, **10**:201 (1942).

20. W.H. Stockmayer, J. Of Chemical Physics, **9**:398 (1942).

21. S. Singh, H. Singh, Physica A, **87**:344-353 (1977).

22. A. Vetere, Chemical Engineering Science, **46**:1787 (1991).

23. J.E. Ramos, F. del Rio, I.A. McLure, Journal of Physical Chemistry B., **102**:10576 (1998).

24. J.H. McFall, D.S. Wilson, L.L. Lee, Ind. Eng. Chem. Res., **41**:1107 (2002).

25. R. Coterman, B.J. Schwarz, J.M. Prausnitz, AIChE Journal, **32**:1787 (1986)

26. D. Gupta, P.T. Eubank, J. Chem. Eng. Data, Vol. 42:961 (1997).

27. G.A. Iglesias-Silva., K.R. Hall, Ind. Eng., Chem. Res., 40:1968 (2001).

28. K. Tsonopoulos, AIChE Journal, **24**:1112 (1978).

29. K. Tsonopoulos, AIChE Journal, **20**:263 (1974).

30. H. Orbey, J.H. , Vera, AIChE Journal, **29**:107 (1983).

31. K. Tsonopoulos, J.H. Dymond, Fluid Phase equilibria, **133**:11 (1997).

32. M.-J. Lee, J.-T. Chen, Journal of Chemical Engineering of Japan, **31**:518, (1998).

33. E.M. Besher, J., Lielmez, Thermochimica Acta, **200**:1 (1992).

34. W.-H. Xiang, Chemical Engineering Science, **57**:1439 (2002).

35. K. Tsonopoulos, J.L. Heideman, Fluid Phase Equilibria, **57**:261 (1990).

TABLES

Table 1. Experimental results and values calculated with JZG-LG model [5-8] for R125. ρ_l denotes initial density.

R125	T_{exp} (K)	B_{exp} (cm^3/mol)	ρ_l (mol/dm^3)	B-LG	RD
1	303.15	-350.7	0.83230	-339.5	-0.03194
2	303.15	-350.9	0.83492	-339.5	-0.03249
3	323.16	-301	0.78813	-300.7	-0.001
4	323.16	-299.8	1.29329	-297.4	-0.00801
5	323.16	-299.5	1.47232	-296.5	-0.01002
6	343.16	-259	3.23418	-260.9	0.007336
7	343.16	-258.8	3.42777	-260.9	0.008114
8	343.16	-259.3	3.13501	-260.9	0.00617
9	363.14	-223.4	2.50984	-234	0.047449
10	363.16	-222.5	3.20336	-233.7	0.050337

Table 2. Experimental results and values calculated with JZG-LG model [5-8] for CO_2. ρ_l denotes initial density.

CO_2	T_{exp} (K)	B_{exp} (cm^3/mol)	ρ_l (mol/dm^3)	B-LG	RD
1	283.14	-136.2	2.24627	-142.6	0.04699
2	283.14	-136.6	2.53439	-142.6	0.043924
3	283.14	-136.4	2.57016	-142.6	0.045455
4	303.15	-118.9	3.28011	-124.5	0.047098
5	303.15	-118.1	3.1186	-124.5	0.054191
6	303.15	-119.2	3.2741	-124.5	0.044463
7	303.15	-118.9	3.3013	-124.5	0.047098
8	313.15	-109.8	2.80884	-117.5	0.070128
9	323.16	-103.6	2.81253	-110.7	0.068533
10	323.16	-103.7	2.87813	-110.7	0.067502
11	333.63	-95	2.49594	-104.4	0.098947
12	333.63	-94.5	2.54126	-104.4	0.104762
13	343.15	-88.7	2.34421	-98.9	0.114994
14	343.15	-90.2	2.47549	-98.5	0.092018

Table 3. Experimental results and values calculated with JZG-LG model [5-8] for CO_2+R125. $x(CO_2)$ and ρ_1 denote the mole fraction of CO_2 and the initial density, respectively.

CO_2+R125	T_{exp} (K)	$x(CO_2)$	B_{exp} (cm^3/mol)	ρ_1 (mol/dm^3)	*B*-LG	RD
1	323.15	0.4434	-196.2	1.88006	-205.7	0.04842
2	323.15	0.6458	-156.8	3.04292	-165.3	0.054209
3	323.15	0.7326	-141.1	1.78731	-147.6	0.046067
4	323.15	0.7327	-141.2	1.71959	-147.6	0.045326
5	323.15	0.8451	-121.5	2.59443	-124	0.020576
6	323.15	0.857	-121.8	2.35075	-121.5	-0.00246
7	323.15	0.8766	-118.9	2.37981	-117.3	-0.01346
8	343.15	0.341	-188.9	1.65300	-192.3	0.017999
9	343.15	0.3919	-177.6	1.98575	-191.6	0.078829
10	343.15	0.6352	-134.7	1.26469	-141.4	0.04974
11	343.15	0.7345	-122.9	1.83107	-130.4	0.061025
12	363.15	0.3693	-155.5	1.67459	-175	0.125402
13	363.15	0.4617	-142.2	1.84847	-160	0.125176
14	363.15	0.6792	-110.4	1.43108	-125.4	0.13587
15	363.15	0.7329	-103.1	1.85933	-116.1	0.126091

Table 4. Experimental results and values calculated with JZG-LG model [5-8] for R32. ρ_1 denotes initial density.

R32	T_{exp} (K)	B_{exp} (cm^3/mol)	ρ_1 (mol/dm^3)	*B*-LG	RD
1	303.15	-284.3	0.7727	-277.5	-0.02392
2	303.16	-283.5	0.93677	-277	-0.02293
3	313.15	-257.5	1.29402	-260.4	0.011262
4	313.16	-257.4	0.83116	-261.6	0.016317
5	323.16	-238.7	1.85209	-245	0.026393
6	323.16	-238.3	1.12925	-245	0.028116
7	333.16	-220.8	0.95137	-238.8	0.081522
8	343.16	-203.2	2.46554	-219.2	0.07874
9	343.16	-202.3	2.68047	-219.2	0.083539

Table 5. Experimental results and values calculated with JZG-LG model [5-8] for R32+CO_2. x(R32) and ρ_l denote the mole fraction of R32 and the initial density, respectively.

R32+CO_2	T_{exp} (K)	x(R32)	B_{exp} (cm^3/mol)	ρ_1 (mol/dm^3)	B-LG	RD
1	303.15	0.1667	-133	2.69036	-126.6	-0.04812
2	303.15	0.3192	-151.5	2.38407	-150.2	-0.00858
3	303.15	0.4576	-171.3	1.59220	-173.5	0.012843
4	303.15	0.6462	-204	1.21316	-206.2	0.010784
5	313.15	0.322	-142.1	2.26684	-141.9	-0.00141
6	313.15	0.4628	-157.8	1.63915	-164.1	0.039924
7	313.15	0.6312	-184.5	1.13067	-192.6	0.043902
8	313.15	0.8029	-219.1	1.14312	-222.9	0.017344
9	323.15	0.3108	-130.3	2.76090	-132.4	0.016117
10	323.15	0.3487	-135	1.83778	-139.6	0.034074
11	323.15	0.5709	-165	1.59316	-171.5	0.039394
12	323.15	0.5866	-167.3	1.69782	-173.8	0.038852
13	333.15	0.3222	-122	1.00300	-127	0.040984
14	333.15	0.4489	-136.6	2.12435	-143	0.046852
15	333.15	0.5791	-153.9	1.64310	-163.2	0.060429
16	333.15	0.7362	-178.5	1.31673	-188.1	0.053782
17	343.15	0.321	-110.5	1.74356	-119.2	0.078733
18	343.15	0.4956	-132.5	1.41187	-142.9	0.078491
19	343.15	0.6856	-157.6	0.91172	-171	0.085025
20	343.15	0.7927	-161.4	1.38575	-179	0.109046

Figure Captions:

Fig. 1. Schematic view of the experimental apparatus.

Legenda:

1 Nitrogen reservoir
2 Vacuum pump (Vacuubrand, mod. RZ2)
3 Precision pressure controller (Ruska, mod. 3981)
4 Gas lubricated dead weight gage (Ruska, mod. 2465)
5 Vibr. cylinder pressure gage (Ruska, mod. 6220)
6 Digital temperature indicator (Corradi, RP 7000)
7 Electronic null indicator (Ruska, mod. 2416)
8 Stirrer
9 Heater
10 Cooling coil connected with an auxiliary bath
11 Differential press. transducer (Ruska, mod. 2413)
12 Measurement chamber (V_A)
13 Expansion chamber (V_B)
14 Magnetic recirculating pump
15 Pt resistance thermometer (Tersid, Pt 100)
16 Vacuum pump for V_B (Vacuubrand, mod. RZ2)
17 Charging fluid reservoir
18 Pt resistance thermometer (Hart Scientific, Pt 25)
19 Digital pressure indicator (Ruska, mod. 7000)
V_1,V_2,V_3,V_4 Constant volume valves

FIGURES

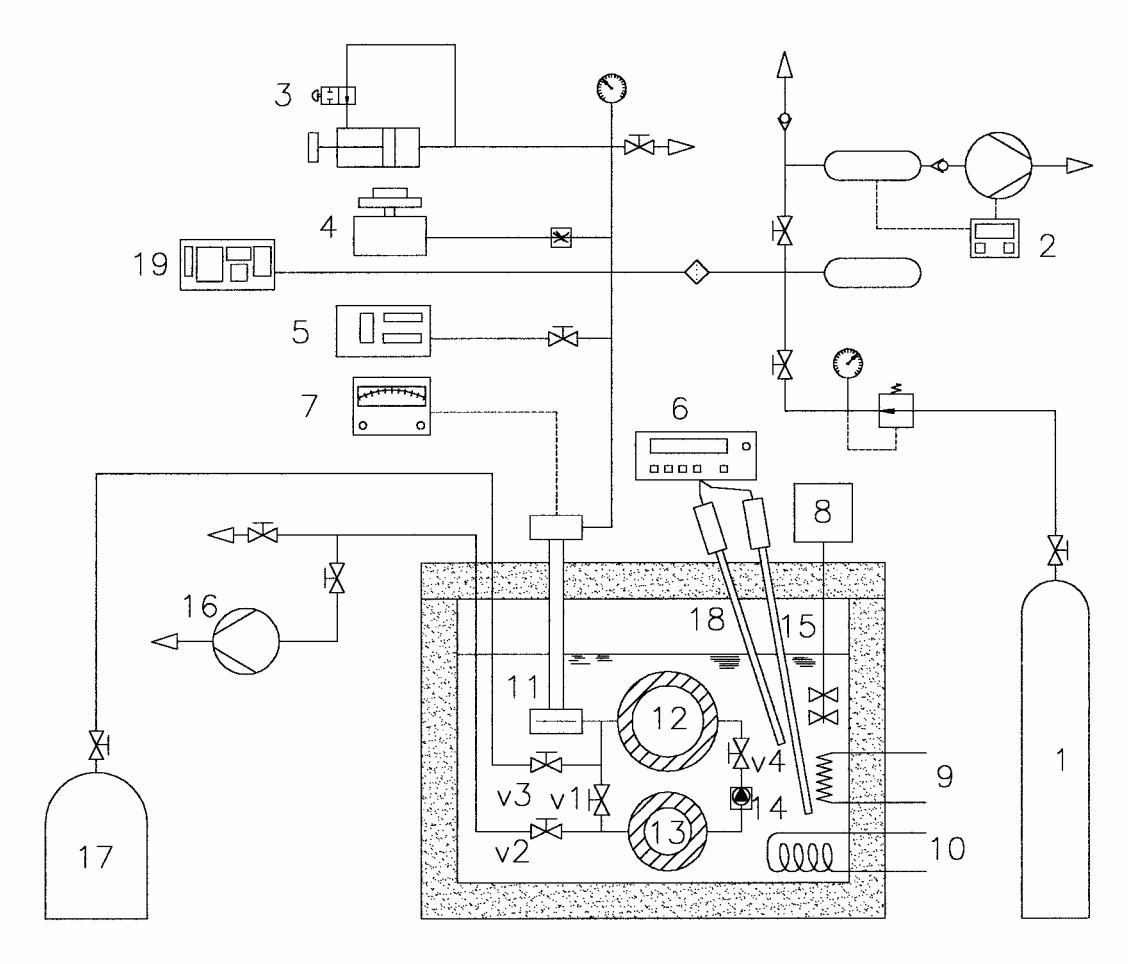

Figure 1. Schematic view of the experimental apparatus.